# A Chemical and Photophysical Analysis of a Push-Pull Compound

A Major Qualifying Project Report:

Submitted to the Faculty

of the

WORECETER POLYTECHNIC INSTITUTE

In partial fulfillment of the requirements for the

Degree of Bachelor of Science

By

Anthony Salerni

Approved:

Prof. Robert E. Connors, Major Advisor

Prof. Christopher R. Lambert, Co-Advisor

## Abstract

A carbazolyl-oxazolone derivative dye (4-(9-hexyl-9H-carbazole-3-ylmethylene)-2-(4-nitrophenyl)-4H-oxazol-5-one) belongs to a class of push-pull compounds, typically displaying solvatochromic behavior. Evaluation of the visible absorption and emission properties were carried out in various solvents. The compound showed a strong sensitivity to solvent polarity in the emission spectra, displaying strong, solvent polarity dependent red shifted bands. Behavior in protic solvents differed from aprotic solvents, with lower emission intensity and a smaller polarity dependent red shift seen in the protic solvents. All absorbance corresponding to the $S_0$ to $S_1$ transition took place between 451-483nm and corresponding fluorescence between 520-682nm. Lifetime decay and fluorescence quantum yields were recorded showing increasing fluorescence lifetime with increasing polarity. The relative quantum yield reaches a maximum in Tetrahydrofuran relative to the other solvents used in this study. During the study, it was determined that the oxazolone moiety was prone to ring opening reactions, resulting in no charge transfer, with absorption and fluorescence occurring in the carbazole moiety.

## Acknowledgements

I would like to acknowledge Professor Robert E. Connors and Professor Christopher R. Lambert for never letting me become too complacent and always pushing towards perfection. Their motivation and guidance helped teach me more than I could have expected before starting this research. My experiences during this project have made me a much richer person.

# Table of Contents

## List of Equations



## List of Tables

# Table of Figures

## Introduction

Many chromophores are organic compounds that contain conjugated pi systems, which absorb a frequency of electromagnetic radiation corresponding to the molecule's transition to higher energy electronic states. This interaction between the electric fields of the molecule and the photon causes electrons from the highest occupied molecular orbital (HOMO) to occupy the lowest unoccupied molecular orbital (LUMO) **[1]**. When the molecule is an excited singlet state, the spin multiplicity of the two unpaired electrons will be opposed. The molecule can undergo a non-radiative process called intersystem crossing, which results in a parallel spin multiplicity of the two unpaired electrons, giving way to a triplet state.

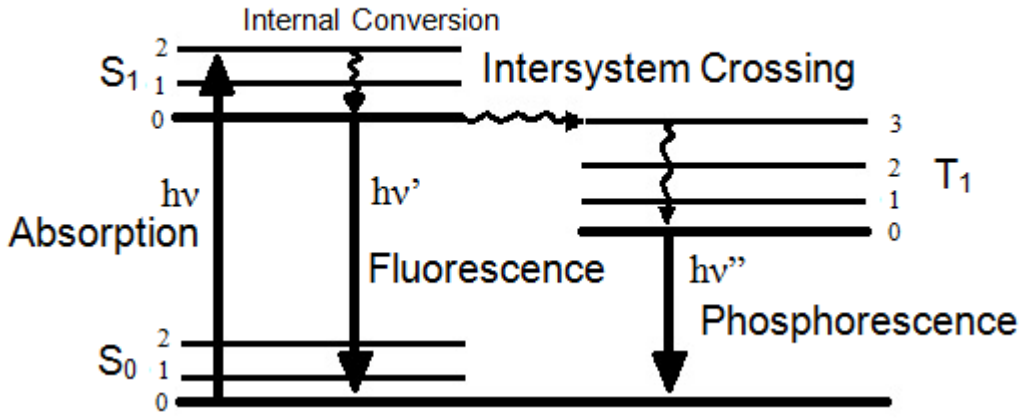


Figure 1: A Jablonski diagram displaying typical modes of absorption, radiative, and non-radiative decay

As the molecule relaxes back down to the ground state, the decay of the molecule will be either radiative or non-radiative. When the molecule undergoes an excitation to a higher electronic state that is not the $S_1$, there is a rapid non-radiative internal conversion and emission of thermal energy when the molecule decays to the lowest excited state. The molecule can continue the non-radiative internal conversion process to the ground state, giving off heat. Radiative decay is observed when molecules in the lowest excited singlet and triplet states undergo fluorescence and phosphorescence,

respectively. With both fluorescence and phosphorescence there is an emission of photons of a particular wavelength corresponding to the energy gap between excited and ground states. Electron correlation between two electrons with parallel spins results in the energy of triplet states being lower to that of singlet states, thus phosphorescence occurs at longer wavelengths than fluorescence **[1]**.

The fluorescence quantum yield is a measurement of the amount of photons which a molecule absorbs, compared to the number of photons emitted **[1]**. Quantum yield can be defined by the rates of radiative and non-radiative processes of the chromophore (Eq.1). When observing fluorescence with respect to time, exponential decays are observed as a molecule returns to the ground state. The fluorescence decay typically lasts between 1 and 10 nanoseconds **[2].** The fluorescence lifetime can be defined by the rates of the radiative and non-radiative processes of a molecule (Eq. 2). Along with quantum yields, lifetimes provide critical data when analyzing the photophysical properties of fluorescent compounds.

$$Q = \frac{k_r}{k_r + k_{nr}}$$

**Equation 1: Definition of Quantum Yield. Q is quantum yield, $k_r$ is the rate of radiative process, and $k_{nr}$ is the rate of non-radiative processes**

$$\tau = \frac{1}{k_r + k_{nr}}$$

**Equation 2: Definition of fluorescence lifetime. τ is lifetime, $k_r$ is the rate of radiative process, and $k_{nr}$ is the rate of non-radiative processes**

The dye under scrutiny, 4-(9-hexyl-9H-carbazole-3-ylmethylene)-2-(4-nitrophenyl)-4H-oxazol-5-one (Cz-OXA-NB), was designed with two main moieties, a carbazole unit, and an oxazolone (Oxazol-5-(4H)-ones) ring substituted at $C_2$ with a nitro-phenyl group. Many carbazole derivatives are used in optical materials due to their various and well-researched photochemical, electrical and photophysical properties **[3].** Carbazole compounds have also exhibited good charge transfer

properties, and have demonstrated the ability to serve as a donor group **[3,4]**. Oxazolones are small cyclic molecules used widely in the fields of chemistry and biology for their multiple reactive sites **[5].** The photophysical and photochemical properties of oxazolones have also been utilized in the use of semiconductor devices, charge transport materials for electro-photographic photoreceptors, and non-linear optical (NLO) materials **[6]**. However, due to the reactive nature of oxazolones they often have poor photochemical stability, being subject to ring-opening reactions in solution **[5]**.

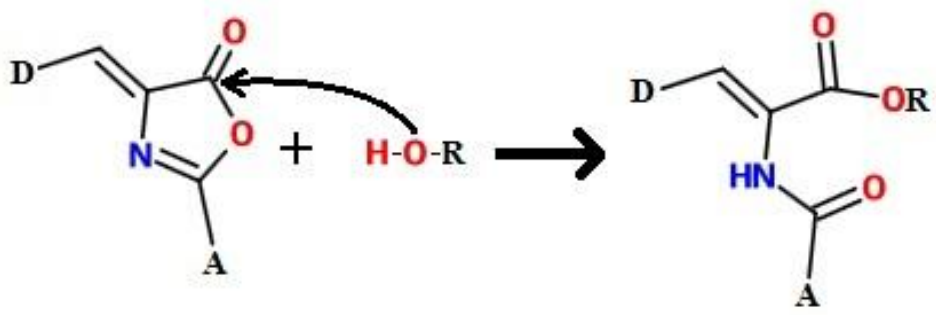


Figure 2: Ring opening reaction of Oxazolone [7].

Cz-OXA-NB was suggested as a solvatochromic material with push-pull properties. The term push-pull refers to the transferring of electron density from the electron donating carbazolyl moiety to the 2-(4-nitrophenyl)-oxazol-5H-one electron withdrawing moiety, also called intramolecular charge transfer (ICT). Excitation of a chromophore to an ICT state results in a significant change in dipole moment.

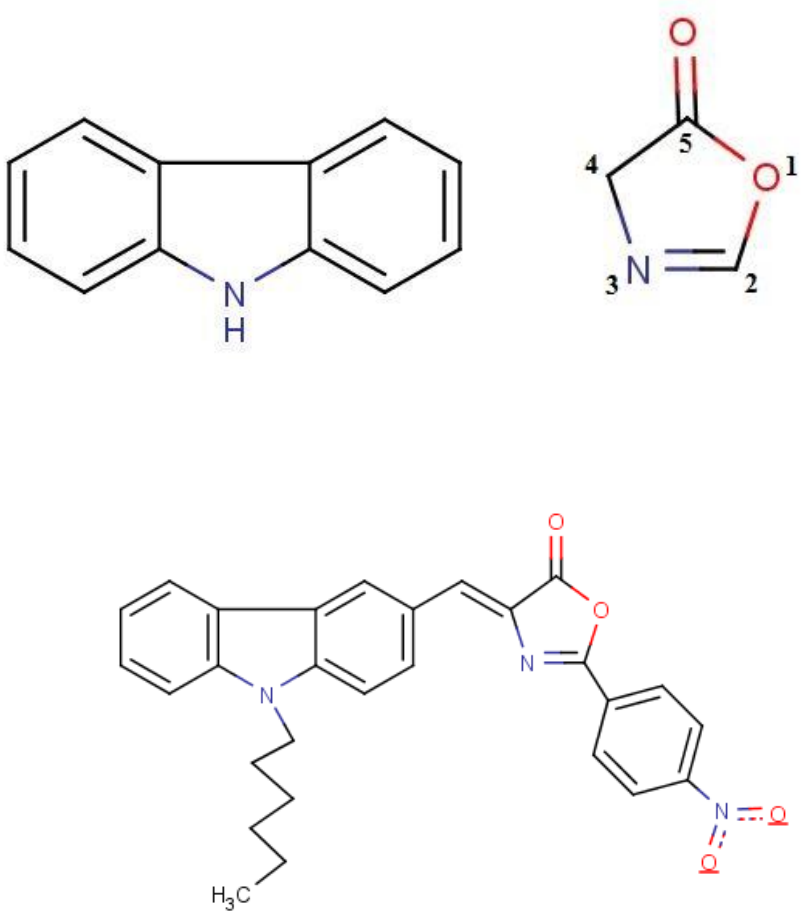


Figure 3: Structures of carbazole (left), oxazolone (right) and Cz-OXA-NB (bottom)

The change in charge distribution causes solvent molecules to undergo reorganization, reorienting to fit the new electronic configuration of the chromophore. The polarity of the solvent molecules can help to stabilize or destabilize the ground and excited states of a chromophore during the solvent relaxation. This process is responsible for solvatochromic behavior, in which the absorption and emission maxima observed in spectra are shifted to higher or lower energy.

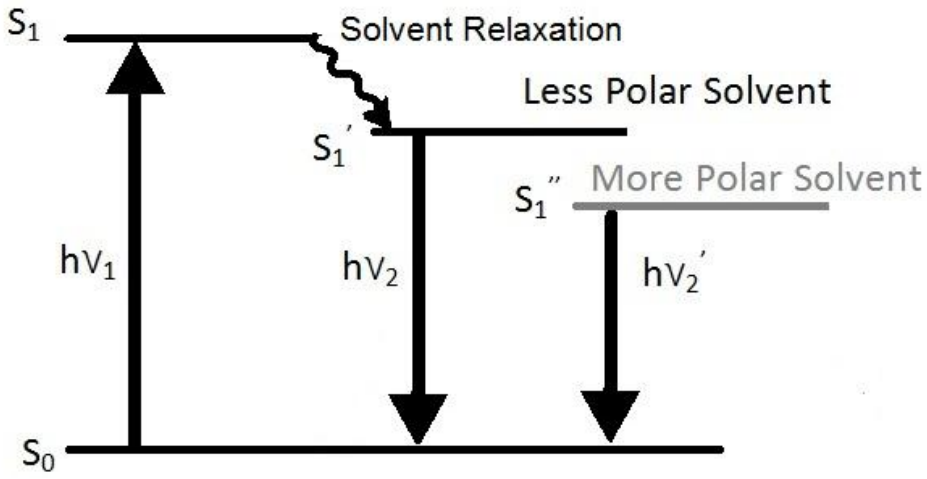


Figure 4: A Jablonski diagram adjusted to show stabilizing solvent effects (S1' and S1)

Solvent polarity can be measured in many different ways; one of the most common is the solvent dielectric constant (ε). Dielectric constant is a measurement of the relative permeability, or the amount of electrical energy stored in the electric field of a solvent. The $E_T(30)$ solvent polarity scale is another popular measurement of solvent polarity. The $E_T(30)$ scale was modeled around the solvatochromic effects of solvent polarity on a betaine dye with respect to the $S_0$ to $S_1$ transition **[2]**. The $E_T(30)$ scale is useful in determining solvatochromic behavior when fluorescence and absorption maxima are plotted against the $E_T(30)$ scale.

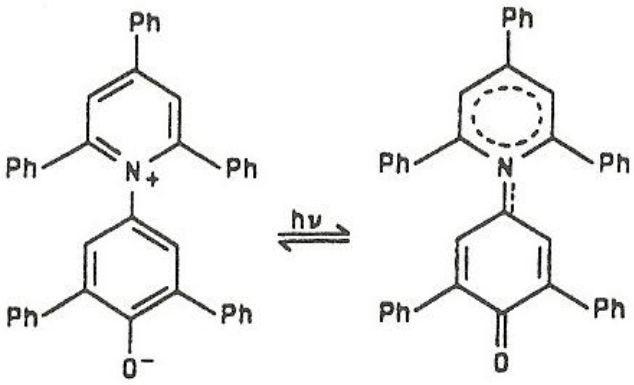


Figure 5: Structure of the betaine dye used as a probe for the $E_T(30)$ scale [8]

Another useful solvent polarity parameter is the solvent orientation polarization function (Δf), which is defined in Eq. 3.

$$\Delta f = \frac{\varepsilon - 1}{2\varepsilon + 1} - \frac{n^2 - 1}{2n^2 + 1}$$

Equation 3: Orientation polarization function equation

In this equation ε represents the solvent dielectric constant and *n* the refractive index. The first part of the equation accounts for the reorientation of the dipole and electrons of the solvent molecule. The second part only accounts for the reorientation of the electrons **[2]**. This solvent polarity parameter is useful in determining the effect of solvent dipole on a chromophore.

If favorable, a chromophore in the ICT state, can undergo twisting of the moieties to provide better charge dispersion. This excited state with new geometry is called a twisted intramolecular charge transfer (TICT) state. TICT states imply two main properties, a charge transfer involving a large dipole moment, and a change in the geometry of a molecule from planar to twisted **[8]**. TICT states tend not to show up in absorbance due to the ground state optimization of the geometry and the Frank-Condon principle, in which excitation occurs instantaneously. In fluorescence many TICT states show duel emission of molecules in both the ICT and TICT states, however this type of luminescence is not seen in every TICT state compound **[8]**. Since there is a mechanical motion of bonds in the formation of TICT states, it has been suggested that viscosity plays a role in TICT states forming, as high molecular interactions will limit non-radiative processes **[9]**.

# Methods

## General

Known concentrations of Cz-OXA-NB were prepared in various solvents. Absorption was measured using a Shi-UV 2100 photospectrometer. The UV-Vis instrument uses mirrors to direct the light from the UV and visible light through two separate slits. The light passing through these slits is directed towards a sample cuvette, and a cuvette containing the reference solvent. The light passing through the sample is measured by a photometer, which determines the relative intensity of the light absorbed at each wavelength.

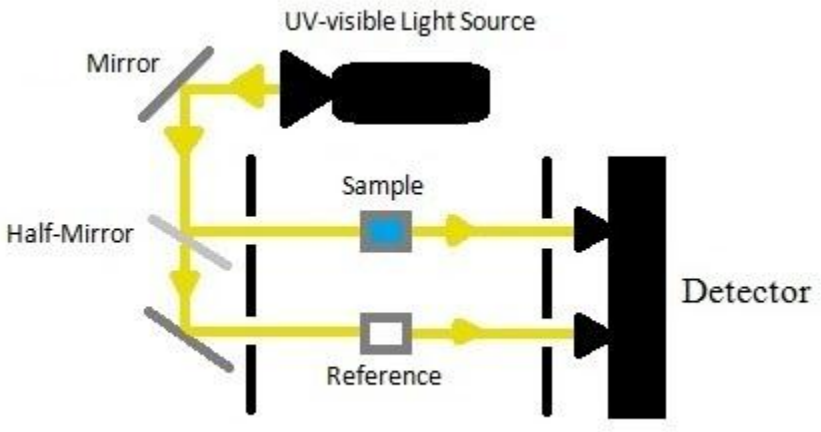


Figure 6: A visible description of the instrumental set up for a UV-Vis photospectrometer

Fluorescence emission spectra were measured on a PerkinElmer LS 50B luminescence spectrometer. The solutions of Cz-OXA-NB were placed in a fluorescence cuvette, clear on all four sides. The instrument was tuned to the excitation wavelength corresponding to the $S_0$ to $S_1$ of Cz-OXA-NB in each solvent to produce the emission spectrum. The fluorescence spectrometer works similarly to absorption, with a few differences. The light source is filtered through a monochromator, to target the desired excitation wavelength. The light travels through a slit into the

sample. Perpendicular to the incident beam another monochromator is used to measure the wavelength of light emitted by the sample. The path lengths of all cuvettes used were equal to 1cm.

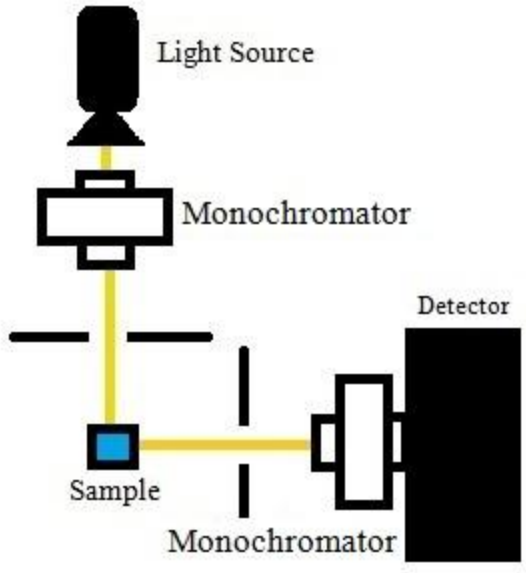


Figure 7: A visible description of the instrumental set up of a fluorescence spectrometer

## Fluorescence Quantum Yield

The relative fluorescence quantum yield was measured using a comparative method. The relative quantum yield refers to a ratio between the solution that yields the highest, and that of all other solutions of different solvent. Cz-OXA-NB was dissolved in each solvent before the absorbance was measured. To ensure that Cz-OXA-NB fully dissolved in solution, acetone was used as a co-solvent, thus the other solvents contained an acetone impurity equal to less than 1%. The solutions were then diluted to a target absorbance of .3 (+/- .015). The emission spectra of all diluted solutions of Cz-OXA-NB in various solvents were measured, having all been excited at a wavelength of 465nm. The resulting $S_1$ to $S_0$ emission bands were integrated to obtain a relative value for fluorescence. Ratios between the max fluorescence value and the values in other solvents were taken to obtain a relative quantum yield. True quantum yields were not obtained as a

compound with similar absorption and emission values to use as the quantum yield standard was not found in time. Given a standard, Eq.4 can be used to obtain the true quantum yield.

$$Q=Q_rI/I_r(OD_r/OD)(n^2/n_R^2)$$

Equation 4: Equation used for finding the quantum yield utilizing a known quantum yield standard

In this equation $Q_r$ is the quantum yield of the standard, I and $I_r$ are the integrated values of the emission bands for the sample and standard respectively, OD and $OD_r$ are the optical densities for the sample and the standard, and $n$ and $n_{R\ are}$ the refractive indices of the sample solvent and standard solvent.

## Lifetime Measurements

The solutions of Cz-OXA-NB were diluted to a maximum absorbance of 0.3 before the samples were degassed with diatomic nitrogen gas for 15 minutes. This precaution is taken as chromophores will be quenched if they collide with oxygen gas in solution. Lifetimes were measured using a Photon Technology International GL3300 nitrogen pulse laser and a GL302 dye laser system. Time-resolve fluorescence with lasers is very similar to that of regular fluorescence spectroscopy; however the laser is tuned to the specific excitation wavelength and fired in pulses. Between the laser pulses, emission of the sample is recorded by a monochromator perpendicular to the incident beam.

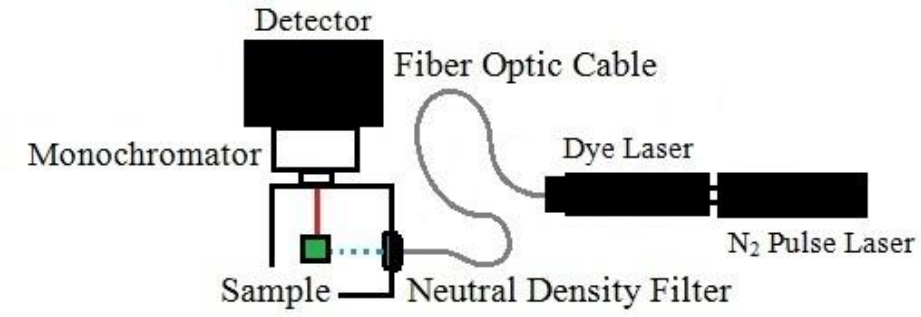


Figure 8: Visible representation of the laser system used to obtain fluorescence lifetimes

Neutral density filters were used to ensure resulting data did not exceed the maximum relative intensity of emission the instrument could detect. LUDOX CL colloidal silica gel (30% weight in water) was initially used to record the instrument response function (IRF) to normalize and correct the fluorescence lifetime data; however in later recording of lifetimes the silica gel was replaced by a solution of non-dairy coffee creamer.

# Results and Discussion

## Analysis of structural

Using Gaussian 09 software, gas phase B3LYP/6-311+G* DFT calculations were performed to investigate structural features of Cz-OXA-NB. The optimized structure shows a small twist at the bridge between the carbazole and oxazolone moieties consistent with reports in the literature **[10]**. The ground state dipole was calculated to be 9.44 Debye.

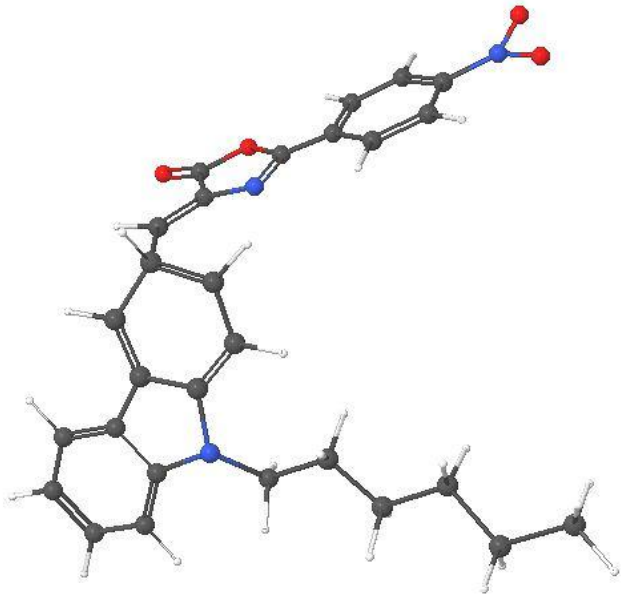

Figure 9: The optimized structure of Cz-OXA-NB in the gas phase

The highest occupied and lowest unoccupied molecular orbitals were also calculated in the gas phase using the Gaussian 09 software (Fig. 10). In the HOMO, a large electron density can be seen favoring the molecule's electron donating carbazole moiety, with an overlap into the oxazolone moiety. This overlap can be attributed to the close proximity of the electron withdrawing carbonyl on the oxazolone. Upon excitation to the $S_1$ state, there is a dramatic shift in electron density, which migrates though the oxazolone portion of the molecule, focusing around the electron

withdrawing nitro phenyl substitution. Thus, the visible polarization of the molecule between HOMO and LUMO states demonstrates the charge transfer nature of the excited state.

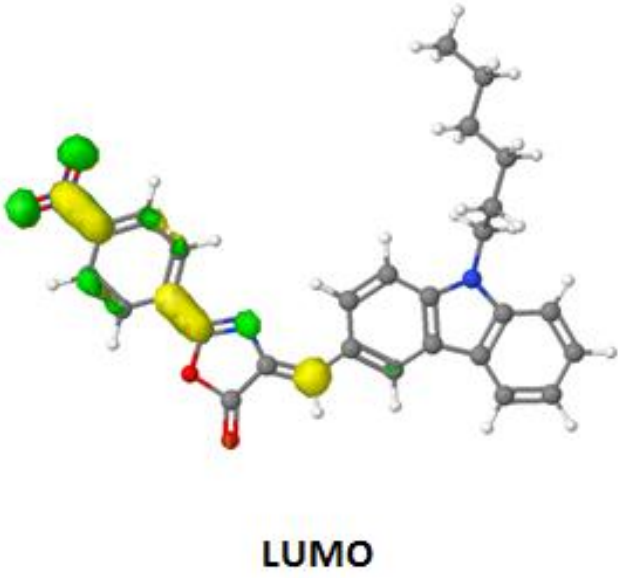

LUMO

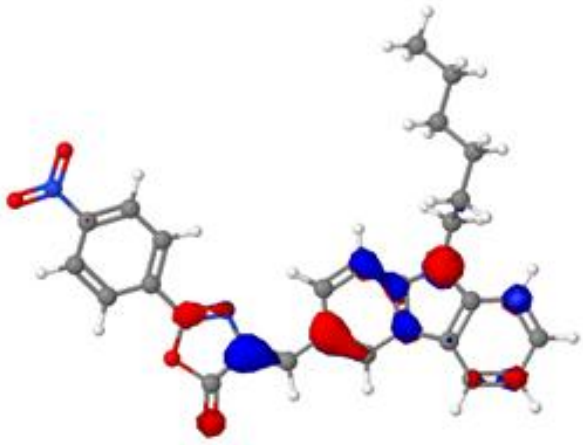

HOMO

**Figure 10: Lowest occupied molecular orbital (top) and highest occupied molecular orbital (bottom) calculated. Electron density represented as blue and red masses in the HOMO and green and yellow masses in the LUMO.**

The strong electron withdrawing nitro group is responsible for driving such a strong charge transfer. The overlap of electron density between the carbazole and oxazolone moieties would make for weaker charge transfer capabilities otherwise.

## Analysis of Spectral Data

UV-visible absorbance of Cz-OXA-NB was measured in various solvents. A summary of the spectral data of Cz-OXA-NB can be seen in table 1. The values for the $S_0$ to $S_1$ transition absorbance maxima differed between 458nm and 483nm, displaying a weak dependence on solvent polarity. Absorbance maxima showed greater sensitivity to the aprotic, protic, and halogenated nature of the solvents. High energy absorbance bands around 260-350nm were seen in many solvents and were attributed to a higher excitation state. These bands became more pronounced in the oxazolone ring-opened Cz-OXA-NB molecule. The cut off range of some solvents made detection of these high energy absorbance bands impossible.

Table 1: Spectroscopic properties of Cz-OXA-NB in various solvents and corresponding polarity parameters

| Solvent | λabs (nm) | λf (nm) | vabs (cm-1) | Vf (cm-1) | Δv (cm-1) | ε | $E_T(30)$ (kcal $mol^{-1}$) | Δf |
|---|---|---|---|---|---|---|---|---|
| n-Hexane | 450 | 520 | 22222.2 | 19230.8 | 2991.4 | 1.88 | 31 | -0.0004 |
| Methyl cyclohexane | 455 | 526 | 21978.0 | 19011.4 | 2966.6 | 2.2 | 31.1 | 0.0195 |
| Carbon Tetrachloride | 475 | 540 | 21052.6 | 18518.5 | 2534.1 | 2.24 | 32.4 | 0.0119 |
| Toluene | 462 | 546 | 21645.0 | 18315 | 3330 | 2.38 | 33.9 | 0.0131 |
| Tetrahydrofuran | 466 | 618 | 21459.2 | 16181.2 | 5278 | 7.58 | 37.4 | 0.2104 |
| Ethyl Acetate | 462.5 | 609 | 21621.6 | 16420.4 | 5201.2 | 6.02 | 38.1 | 0.1996 |
| Chloroform | 483 | 630 | 20703.9 | 15873 | 4830.9 | 4.81 | 39.1 | 0.1491 |
| Dichloromethane | 480 | 650 | 20833.3 | 15384.6 | 5448.7 | 8.93 | 40.7 | 0.2124 |
| Acetone | 465 | 656 | 21505.4 | 15243.9 | 6261.5 | 20.7 | 42.2 | 0.2843 |
| Acetonitrile | 466 | 686 | 21459.2 | 14577.3 | 6882.0 | 37.5 | 45.6 | 0.3054 |
| Isopropanol | 470 | 587.11 | 21276.6 | 17032.6 | 4244.0 | 19.92 | 48.4 | 0.2769 |
| Ethanol | 470 | 591 | 21276.6 | 16920.5 | 4356.1 | 24.55 | 51.9 | 0.2887 |
| Methanol | 468 | 593 | 21367.5 | 16863.4 | 4504.1 | 32.7 | 55.4 | 0.3093 |
| Acetic Acid | 468 | 580.84 | 21367.5 | 17216.4 | 4151.1 | 6.15 | 51.7 | 0.2028 |
| t-Butanol | 473 | 582.5 | 21141.6 | 17166.8 | 3974.9 | 10.9 | 43.3 | 0.2436 |
| Ethylene Glycol | 469 | 615 | 21322.0 | 16260.2 | 5061.8 | 37 | 56.3 | 0.271 |

The weak solvent polarity dependence in the absorption spectra are an indication that while in the ground state, solvent polarity only has a small effect on stabilization of Cz-OXA-NB. The even electron density distribution over the carbazole moiety and overlap into the oxazolone while the molecule is in the ground state coincides with the apparent weak electrical interactions between the solvent molecules and Cz-OXA-NB observed in absorption.

Fluorescence emission spectra of Cz-OXA-NB were also recorded in various solvents. In the non-polar solvents such as n-hexane, fluorescence was seen between 520-550nm with visible vibronic structure. The low interaction between non-polar solvents and the dye in the excited state preserve the vibration structure making observations of such phenomena possible. In more polar aprotic solvents, such as tetrahydrofuran (THF), there is a notable red shift and broadening of the emission band, as the solvent interferes with the molecule, wiping out any vibrational structure. The polarity-dependence of the redshift observed in the emission spectra is very prominent compared to that seen in the absorption spectra, indicating that polar solvents stabilize the excited state. The redshift occurs due to the relaxation of the solvents. During relaxation of the solvents, polar solvents reorient themselves to minimize the energy of the system in response to changes in the electrical properties of Cz-OXA-NB, due to excitation. This polarity dependent redshift seen in fluorescence shows a distinct difference between the Frank-Condon $S_1$ state and the solvent relaxed $S'_1$ state in various solvents, an indication of charge transfer **[8]**.

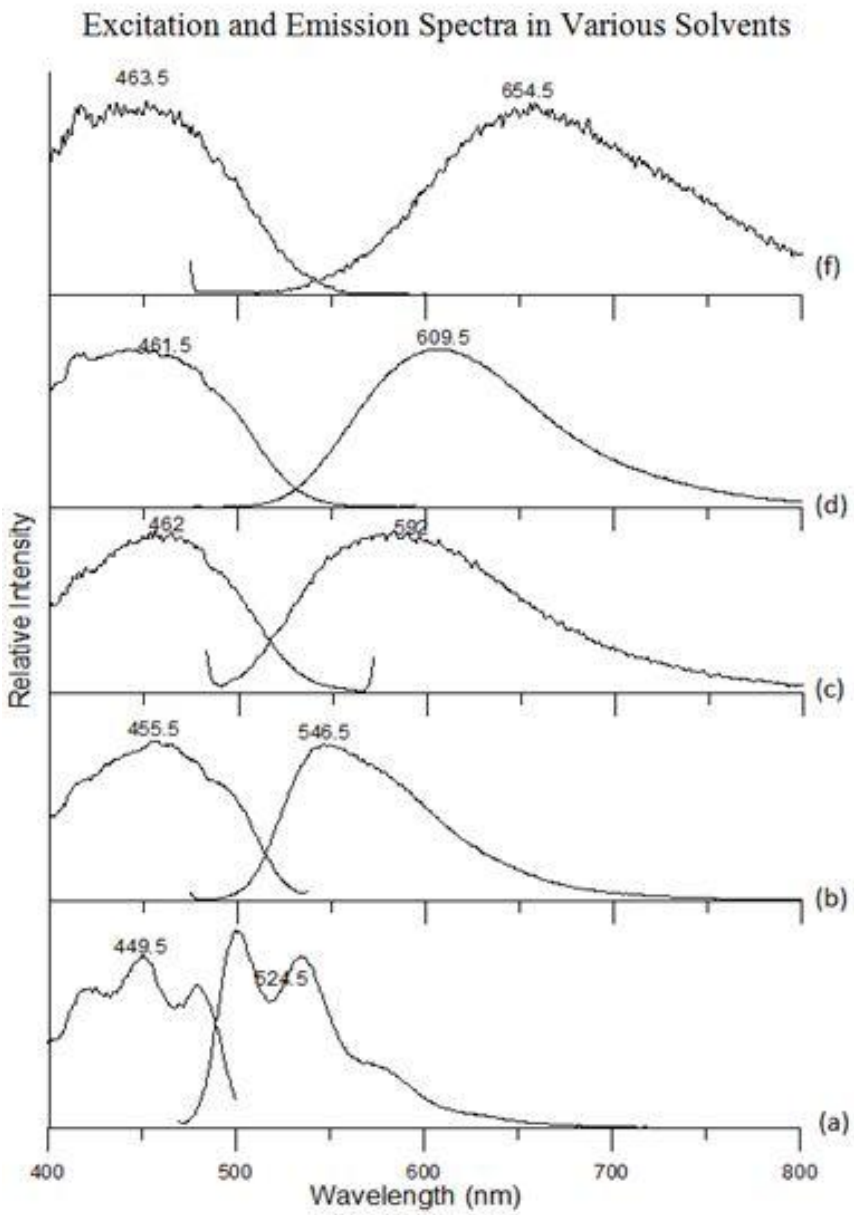


**Figure 11: Excitation and emission spectra of Cz-OXA-NB in solvents of various polarities for the purpose of comparison: (a) n-Hexane (b) Toluene (c) t-Butanol (d) Ethyl Acetate (f) Acetone.**

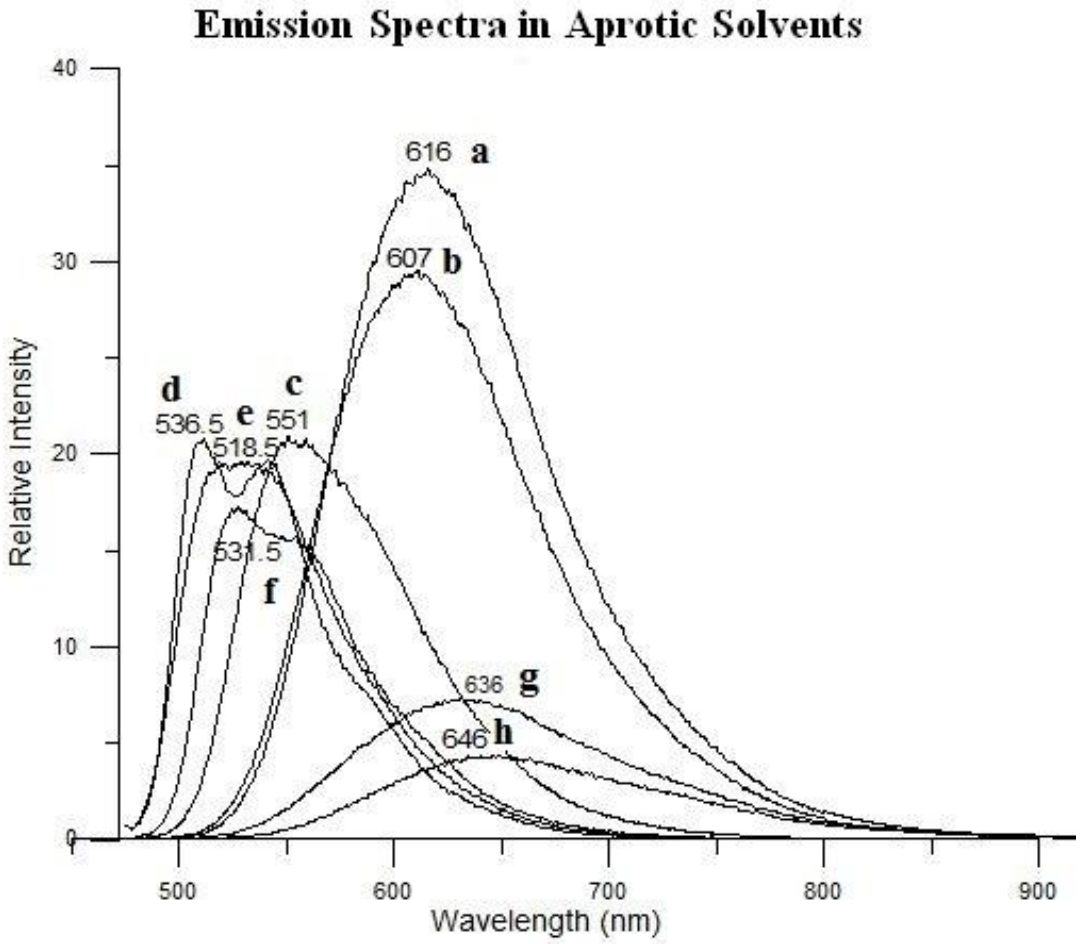


**Figure 12: Emission spectra of Cz-OXA-NB in various aprotic solvents: (a)tetrahydrofuran (b)ethyl Acetate (c)toluene (d)n-hexane (e)methyl cyclohexane (f)CCl4 (g)chloroform (h)dichloromethane.**

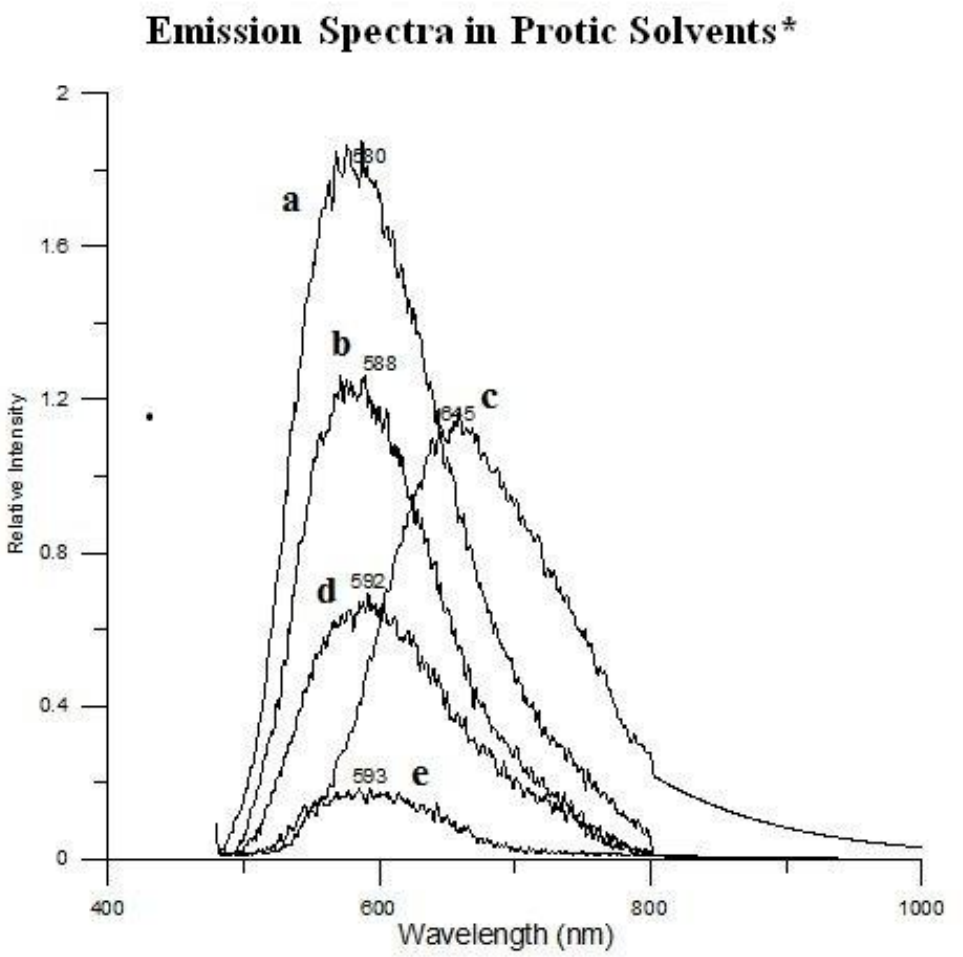


**Figure 13: Emission of Cz-OXA-NB in various protic solvents: (a) acetic acid (b)isopropanol (c)acetone (d)ethanol (e)methanol. *Acetone is not a protic solvent but was grouped together with protic solvents in this plot to compare relative intensities**

The redshift in emission max is clearly visible in Figures 11, 12, and 13, as solvent polarity increases. Different behavior in the emission of protic solvents relative to aprotic solvents is also observed. The decrease in emission intensity of protic and aprotic solvents of higher polarity are due to fluorescence quenching, by either the reduction of the radiative process, or the increase in the non-radiative process.

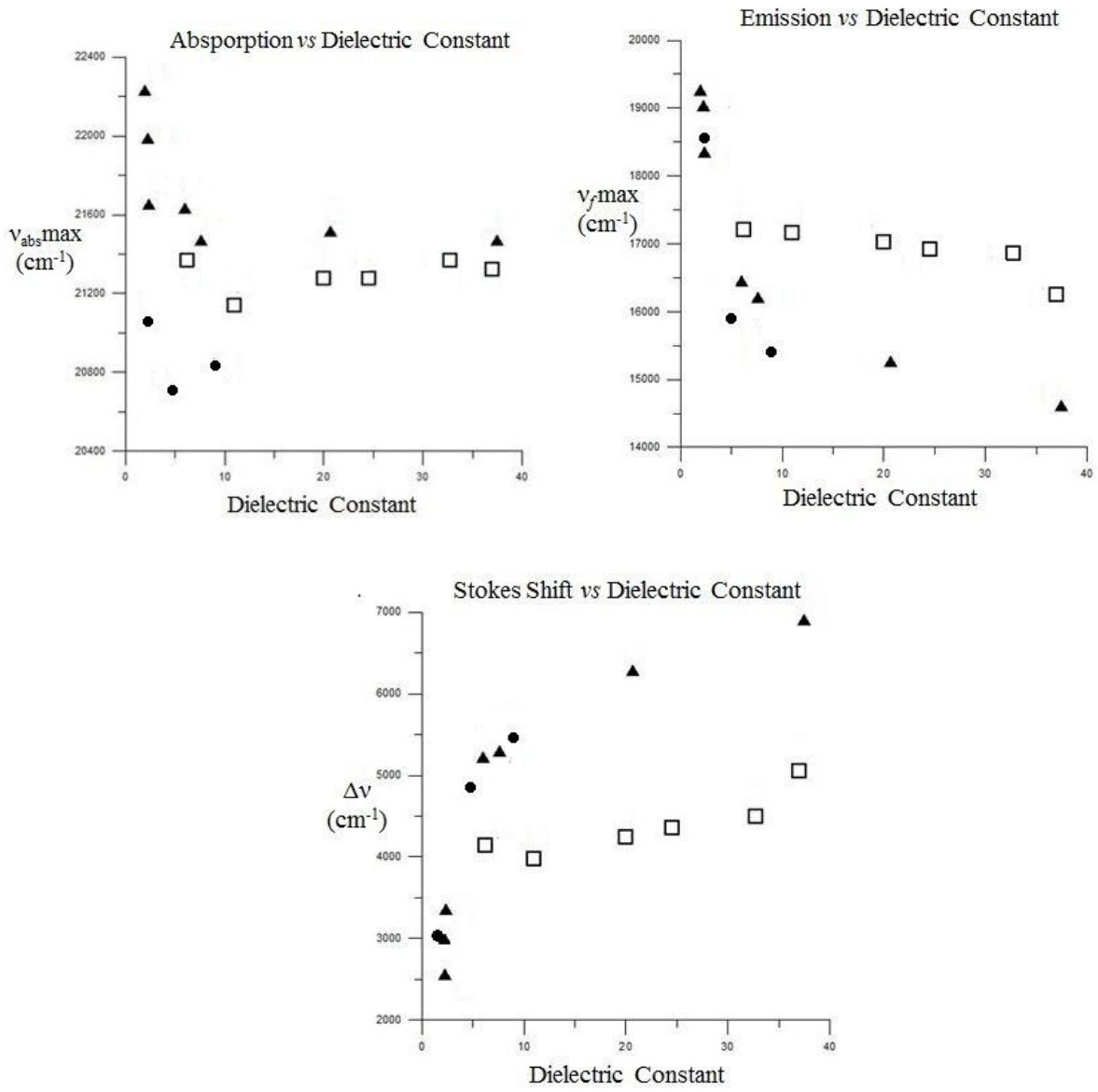


**Figure 14: The absorption (top left) and emission (top right) maxima and stokes shifts (bottom middle) in wavenumbers plotted against the dielectric constant of the solvents. The data is grouped by protic (square), aprotic (triangle) and halogenated (circle) solvents to observe trends.**

The trend seen in the aprotic solvents of the fluorescence max shows Cz-OXA-NB becomes less sensitive to the electric field of the solvent as the solvent dielectric constant increases. A similar trend is seen in the absorption spectra in aprotic solvents with the exception of the halogenated solvents. The behavior in protic solvents is consistently much

less sensitive to the dielectric constant as it does not account for hydrogen bonding effects (Fig. 14).

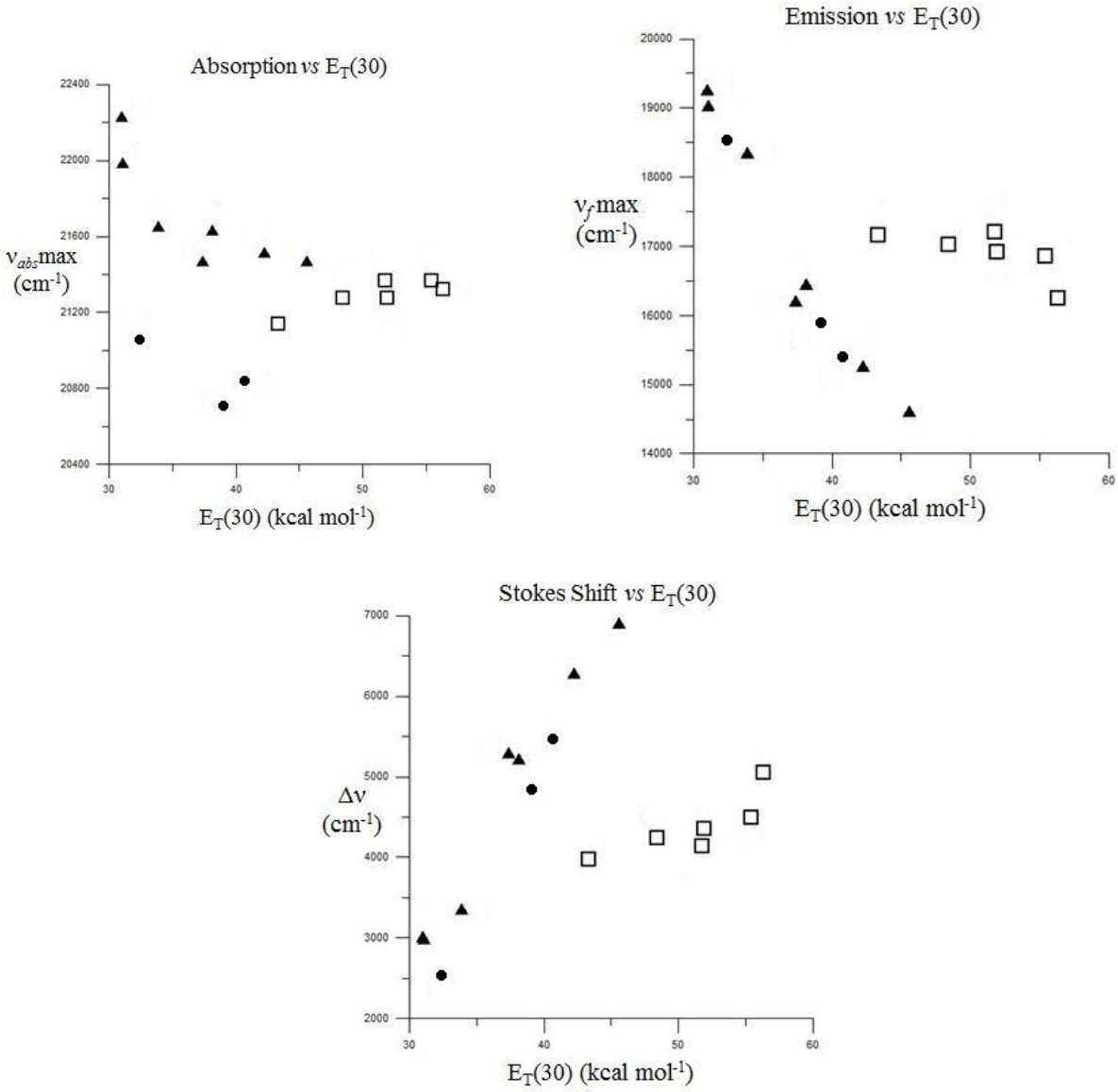


**Figure 15: The absorption (top left) and emission (top right) maxima and stokes shifts (bottom middle) in wavenumbers plotted against the $E_T(30)$ scale of solvents polarity. The data is grouped by protic (square), aprotic (triangle) and halogenated (circle) solvents to observe trends.**

Trends in the behavior of protic and aprotic solvents differ when absorbance and emission maxima are plotted against the $E_T(30)$ solvent polarity scale, as it does not account for hydrogen bonding. Similar to what is seen with dielectric constant, absorption in aprotic solvents show a slight dependency on the $E_T(30)$ value of solvents, with the exception of halogenated solvents.

Linear trends are observed in fluorescence indicating that the redshift in emission is dependent on solvent polarity.

As with both dielectric constant and $E_T(30)$ values, Δf does not account for hydrogen bonding, thus trends in protic and aprotic solvents differ. The reorientation of the solvent dipole shows less of an effect in absorbance compared to other polarity parameters seen previously. Halogenated solvents again have a unique effect on absorption, and the stabilizing effects on the ground state are independent of solvent polarity. The reorientation of the solvent dipole has a stabilizing effect, lowering the energy of the $S_1$ state as solvent polarity increases.

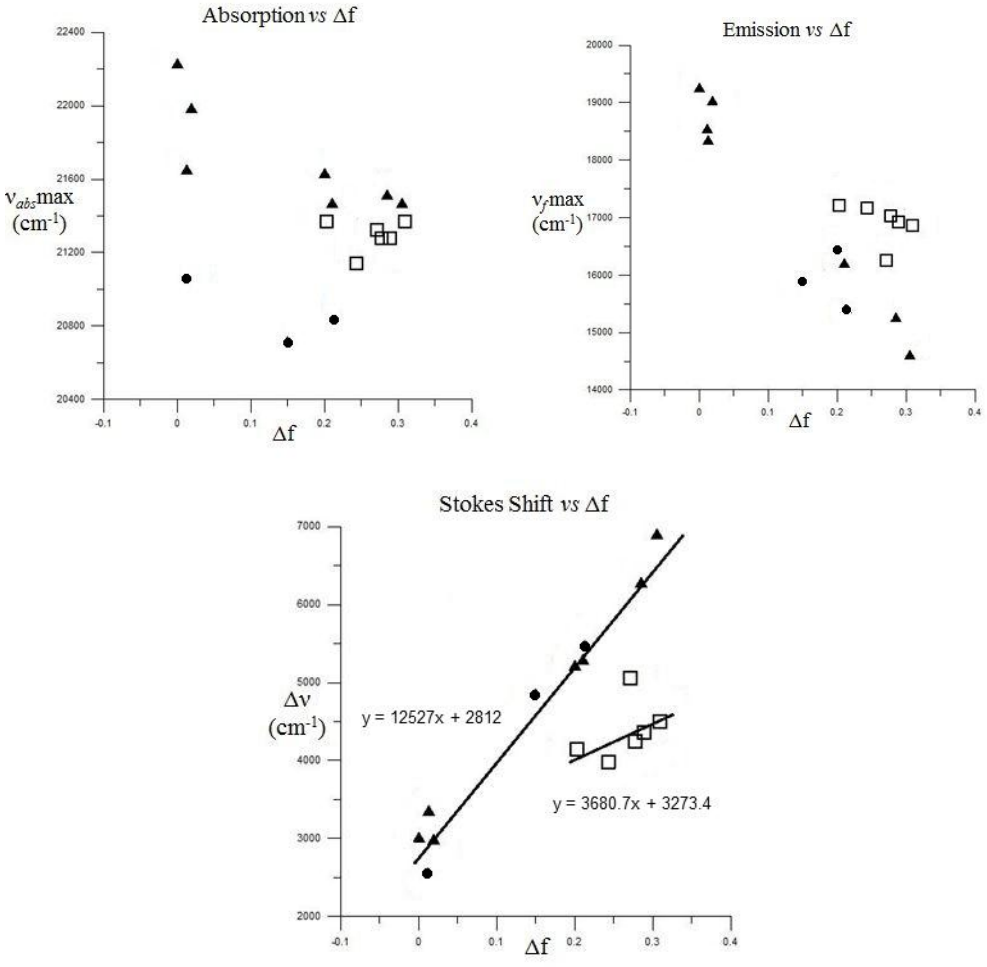


**Figure 16: The absorption (top left) and emission (top right) maxima and stokes shifts (bottom middle) in wavenumbers plotted against the solvent orientation polarization function. The data is grouped by protic (square), aprotic (triangle) and halogenated (circle) solvents to observe trends.**

A linear trend seen in the relationship between Stokes shift and the solvent orientation polarization function, also called a Lippert-Mataga plot, is evidence of charge transfer. The trend seen in the Lippert-Mataga plot can be defined using the Lippert-Mataga equation (Eq. 4)

$$\nu abs_{max} - \nu f_{max} = (2\Delta\mu^2/hca^3)\Delta f + C$$

Equation 5: The Lippert-Mataga equation

where $\Delta\mu$ is the change in dipole moment, h is planks constant, c is the speed of light, *a* is the Onsager's cavity radius, $\Delta f$ is the solvent orientation polarizations function, $\nu abs_{max}$-$\nu f_{max}$ is the stokes shift, and C is a constant representing the y-intercept. Using the slope of the trend line from Fig. 16 to define $[2\Delta\mu^2/hca^3]$ in the Lippert-Mataga equation, the change in dipole was calculated to be 18 D which almost doubles the ground state dipole moment of 9.44 D.

This large change in dipole moment calculated for Cz-OXA-NB coincides with the charge transfer seen by the large shift in electron density between the HOMO and LUMO orbitals calculated by the Gaussian software. The experimental and theoretical data confirm the charge transfer nature of Cz-OXA-NB and reaffirms the idea that during solvent relaxations, the reorientation of the solvent molecules can serve to stabilize the polarized regions of the $S_1$ state in Cz-OXA-NB.

Due to low emission at high polarity, a solvent viscosity experiment was used to determine if low emission was from mechanical non-radiative processes in the excited state of Cz-OXA-NB. Ethylene glycol and acetonitrile were the two solvents chosen for the experiment as their dielectric constants differ by a small amount, 0.3, and viscosities greatly, by 16.55cP. The absorbance of OXA-NB in ethylene glycol was measured to be 469nm, and in acetonitrile to be 467nm. The lack of viscosity effects in absorption is expected due to the Frank-Condon principle, where absorption happens instantaneously. Equal concentrations of Cz-OXA-NB were prepared in acetonitrile and ethylene glycol. The ethylene glycol solution contained a 1% (by volume) impurity of acetonitrile

as Cz-OXA-NB was difficult to dissolve in ethylene glycol due to the viscosity. The emission maximum for acetonitrile was measured to be 682 nm with very low emission intensity, while the emission maximum for ethylene glycol was recorded at 615nm with greater emission intensity comparatively.

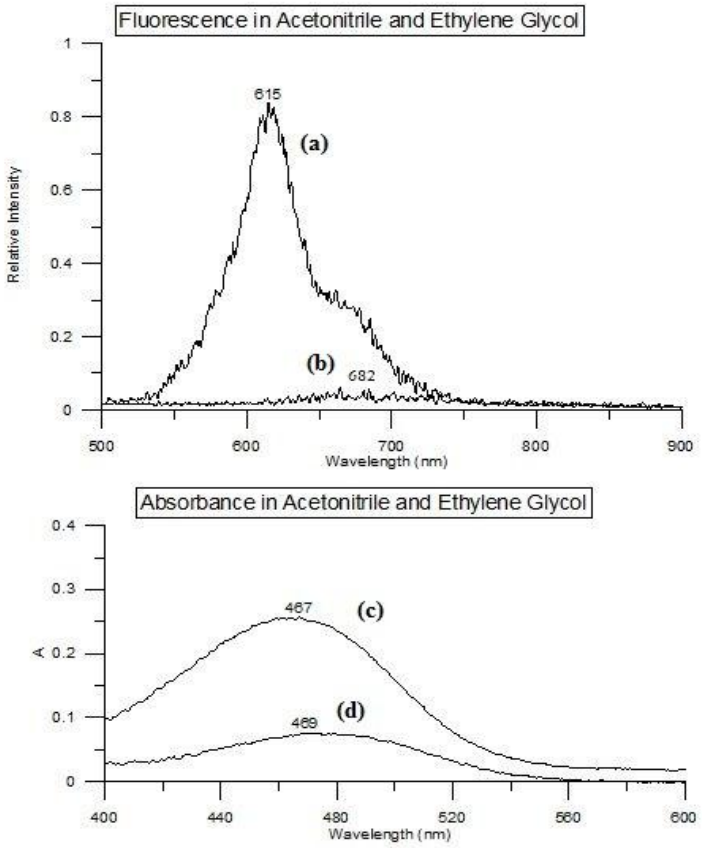


**Figure 17: The emission and absorption of Ethylene Glycol (a and d respectively) and acetonitrile (b and c respectively) for comparison. Concentration of Cz-OXA-NB is equal for both solutions**

The difference in emission maxima of ethylene glycol and acetonitrile does not clearly show that there is a viscosity effect present in the excited state, as behavior in protic and aprotic solvents have already been shown to differ. However the relative intensity of the emission in ethylene glycol is greater than the relative intensity of the emission in the less polar protic solvent methanol. The lower wavelength shoulder of the ethylene glycol emission spectra may be due to a duel emission between two different fluorescent species, such as ICT and TICT states

During experimentation, it was also determined that the oxazolone portion of the compound was prone to a based catalyzed ring opening, resulting in a bleaching of the dye solution. This was first seen using methanol as a solvent, where over time the relative absorbance of the $S_0$ to $S_1$ transition decreased and while UV absorbance at 275nm increased. Cz-OXA-NB in ethylene glycol, which contains two terminal hydroxyl groups on each side of the ethylene, showed the fastest rate of bleaching. In combination with the fact that there was no bleaching seen in tert-butanol, the availability of hydroxyl groups is a main factor in the reactions. A solution of Cz-OXA-NB in tetrahydrofuran was allowed to bleach overtime before a fluorescence spectrum was recorded.

The resulting emission band was hypothesized to be from the carbazole moiety. This was confirmed when the absorbance and fluorescence spectra taken experimentally of 9-vinylcarbazole in THF were compared to the absorbance and fluorescence spectra of bleached Cz-OXA-NB in THF, whose maxima differed by approximately 10nm in both absorbance and emission. Comparison of the absorption and emission spectra of 9-vinylcarbazole and bleached Cz-OXA-NB can be seen in Fig. 18.

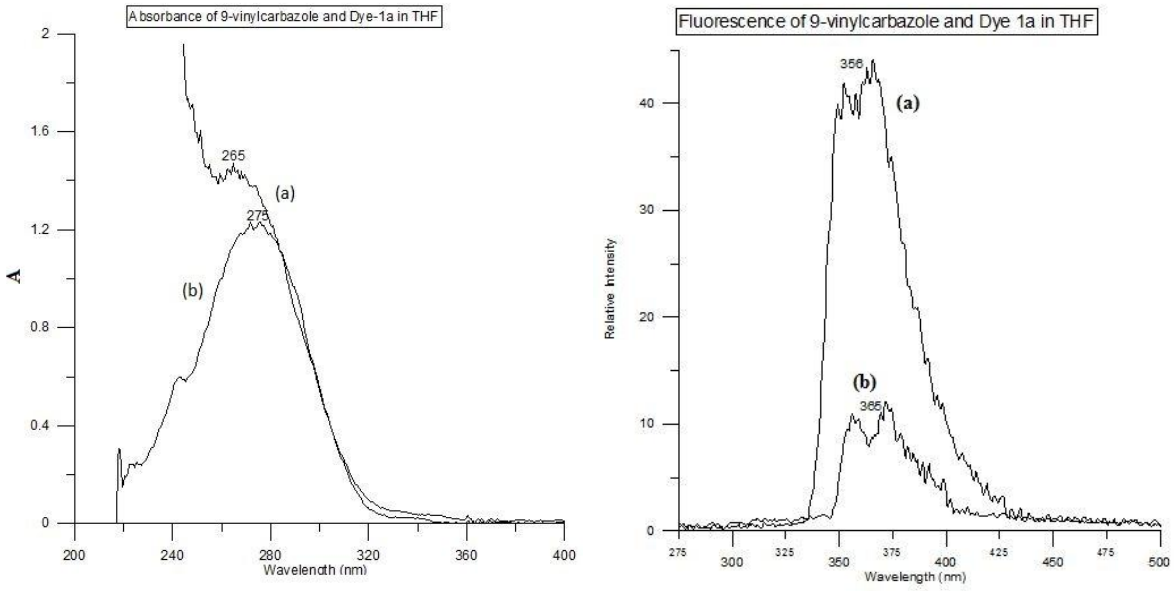


**Figure 18: A comparison of the absorption (left) and fluorescence (right) of 9-vinylcarbazole and oxazolone ring opened Cz-OXA-NB in THF.**

## Photophysical data analysis

The photophysical properties of Cz-OXA-NB in various solvents are listed in table 2. The longer fluorescence lifetime of the longer wavelength emissions of Cz-OXA-NB is not typical of other non-solvatochromic chromophores with low wavelength emissions. In most cases lower wavelength emission are expected to have a shorter lifetime than emissions of shorter wavelength due to the smaller energy gap between the $S_1$ and $S_0$.

Table 2: Photophysical properties of Cz-OXA-NB in various solvents –No data *below the detection of the instrument

| Solvent | $\tau$ (ns) | $\Phi_{rel}$ |
|---|---|---|
| n-Hexane | 0.299 | 0.4061 |
| Methyl cyclohexane | - | 0.3937 |
| Carbon Tetrachloride | - | 0.3888 |
| Toluene | 0.645 | 0.4637 |
| TetrahydroFuran | 1.82 | 1 |
| Ethyl Acetate | 1.43 | 0.8316 |
| Chloroform | - | 0.2970 |
| Dichloromethane | - | 0.1655 |
| Acetone | - | 0.0418 |
| Acetonitrile | - | 0.0048 |
| Isopropanol | <.05* | 0.0564 |
| Ethanol | - | 0.0202 |
| Methanol | - | 0.0050 |
| Acetic Acid | - | 0.0390 |
| t-Butanol | - | - |

In Cz-OXA-NB, the red shifted emission in polar solvents is a sign of stabilization of the excited state by the solvent. This lack of stabilization of the excited state by non-polar solvents allows for faster decay to the ground state by other non-radiative process **[2]**.

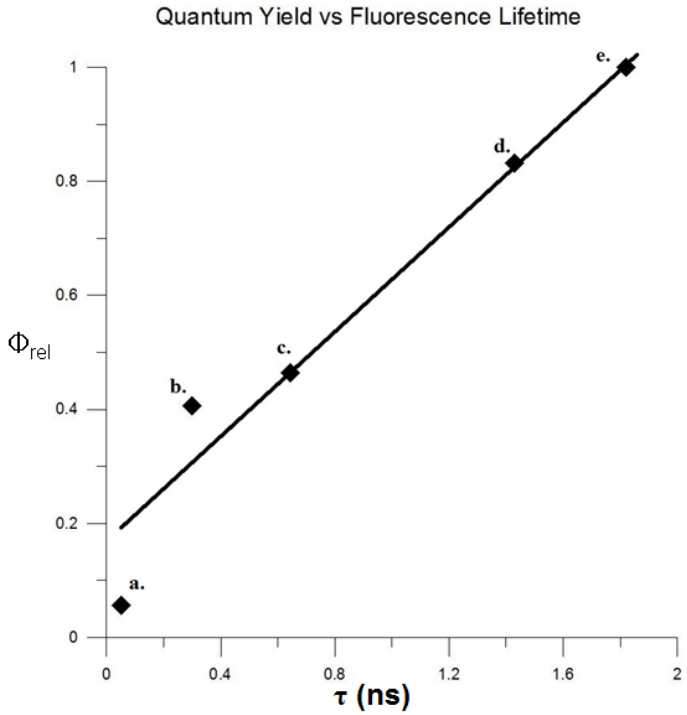


Figure 19: Shows the relation between relative quantum yield and lifetime. (a. isopropanol b. n-hexane c. toluene d. ethyl acetate e. tetrahydrofuran)

The trend seen in Fig. 19 can be defined by the following equation:

$$\frac{k_r}{k_r + k_{nr}} = \frac{m}{k_r + k_{nr}} + C$$

Equation 6: Equation for the trend line seen when relative quantum yield is plotted against fluorescence lifetime

where $k_r$ is the rate of the radiative process, $k_{nr}$ is the rate of non-radiative processes, $m$ is the slope, and $C$ is the y-intercept. This equation can be simplified to:

$$k_r = m + C(k_r + k_{nr})$$

Equation 7: Simplified equation defining the trend line seen when relative quantum yield is plotted against fluorescence lifetime

If given the absolute quantum yield, the trend in Fig. 19 implies that the solvent only has an effect on the rate of the non-radiative processes of Cz-OXA-NB. As of now, the trend line shows that the radiative process $k_r$ is proportional to the slope $m$. The high quantum yield in the polar

aprotic solvent THF confirms that stabilization of the excited state by the polar solvents limits the rate at which non-radiative processes occur. As polarity continues to increase the quantum yield begins to decrease, which indicates either an increase of non-radiative processes, or quenching by the solvent through other processes that decrease or overshadow the fluorescence radiative rate. The quenching of fluorescence is not visibly dependent on the electrical properties due to the behavior seen in the solvent viscosity experiment. The observed effect of solvent viscosity between protic solvents is evidence that high viscosity limits the rate at which non-radiative processes that may quench the radiative process occur.

## Conclusion

Through the analysis of experimental and theoretical data recorded, Cz-OXA-NB was able to be determined to be a charge transfer material with solvatochromic behavior. An increase in stokes shift was seen as solvent polarity increased. The large charge transfer, driven by the nitrobenzene substitution, is seen in the differences between electron densities of the calculated HOMO and LUMO. These theoretical calculations coincide with the 18D change in dipole moment calculated experimentally, confirming the ICT state. Stabilization of the ground state was found to not depend on solvent polarity alone, as the aprotic halogenated solvents produced longer wavelength absorbance maxima compared to the other aprotic solvents. The excited state of Cz-OXA-NB was stabilized by polar solvents, resulting in a redshift seen in the maxima of the emission spectra. Solvent viscosity on the $S_1$ state showed evidence of an effect on the non-radiative rates of Cz-OXA-NB. Low quantum yield in highly polar solvents indicates either the increase in non-radiative processes, or a solvent quenching through some other process.

## Recommendations for Future Work

Future research might try to determine the processes responsible for the fluorescence quenching of Cz-OXA-NB, which could also include experiments to determine the presence of a TICT state. Future research could also determine what other solvent effects contribute to ground state stabilization of Cz-OXA-NB. Evidence of triplet state phosphorescence was seen in low temperature fluorescence spectra of Cz-OXA-NB in chloroform and carbon tetrachloride, meriting further in-depth experimentation and analysis of the potential triplet states properties of Cz-OXA-NB, and would help provide insight into more possible uses for this compound.

## References


1. Barltrop J.; Coyle, J. *Principles of Photochemistry*; John Wiley & Sons Ltd.; 1975
2. Lakowicz, J. R. *Principles of Fluorescence Spectroscopy*; 3rd ed.; Springer: New York, 2006
3. Gundogdu, C., Topkaya, D., Ozturk, G., Alp, S., Ergun, Y. **(2010)** "Synthesis of Novel Carbazolyl-Oxazolone Derivatives and Their Spectroscopic Properties" *J. Heterocyclic Chem.*, **47**, 1450-1453
4. Y, Qian. **(2008)** "3,6-Disubstituted carbazole chromophores containing thiazole and benzothiazole units: Synthesis, characterization and first-order Hyperpolarizabilities" *Dyes and Pigments*, **76**, 277-281
5. Rodrigues, C., Mariz, I., Macoas, E., Afonsa, C., Martinho, J. **(2012)** "Two photon absorption properties of push-pull oxazolone derivatives" *Dyes and Pigments*, **95**, 713-722
6. Ozturk, G., Alp, S., Ergun, Y., **(2007)** "Synthesis and spectroscopic properties of a new 5-Oxazolone derivatives containing an N-phenyl-aza-15-crown-5 moiety" *Tetrahedron Letters*, **48**, 7347-7350
7. Nicholas, E., and Phelps, D. **(1980)** 'Synthesis of Isomeric Methyl- and Dimethyl-substituted 4-benzylidene-2-phenyloxazolin-5-ones and Ring-Opened Derivatives" *Journal of Chemical and Engineering Data*, **25**, 81-90
8. Suppan, P.; Ghoneim, N. *Solvatochromism*; Royal Society of Chemistry; 1997
9. Simon, J., Su, S., **(1990)** 'Effect of Viscosity and rotor Size on the Dynamics of Twisted Intramolecular Charge Transfer" *J. phys. Chem.*, **94**, 3656-3660
10. Diaz, J., Villacampa, B., Lopez-Calahorra F., Velasco, D. **(2002)** "Experimental and Theoretical study of a New Class of Acceptor Group in Chromophores for Nonlinear Optics: 2-substituted 4-Methylene-4H-oxazol-5-ones" *Chem. Mater.*, **14**, 2240-2251